Steered Molecular Dynamics Simulation of the Detaching Process of Two Parallel Surfaces Glued Together by a Single Polyethylene Chain

Yu Wang,[1,2] Linxi Zhang,[1] Jun Cheng[1,3]

[1]*Department of Physics, Wenzhou University, Wenzhou 325027, People's Republic of China*
[2]*Department of Physics, Huzhou University, Huzhou 313000, People's Republic of China*
[3]*Department of Physics, Jinhua University, Jinhua 321007, People's Republic of China*

Received 29 May 2008; accepted 1 November 2008
DOI 10.1002/app.29626
Published online 8 September 2009 in Wiley InterScience (www.interscience.wiley.com).

ABSTRACT: The detaching process of two parallel surfaces glued together by a single polyethylene chain *in vacuo* was investigated with a steered molecular dynamics method. Various statistical properties were analyzed in detail, including the mean-square end-to-end distance; parallel and perpendicular mean-square radii of gyration; shape factor; segment density distribution; average percentages of the microstructure of the chain of the tail, train, bridge, and loop; average surface adsorption energy; average total energy; and average pulling force ($\langle f \rangle$). All these properties depended strongly on the pulling velocity (v). There existed a peak in the curve of $\langle f \rangle$ as a function of the detaching distance. Further, the relation between the maximum value of $\langle f \rangle$ and v showed three distinctive regions: a region of weak dependence at $v < 10^{-2}$ Å/ps, a region of strong dependence at 10^{-2} Å/ps $< v <$ 6.50 Å/ps, and a region of weak dependence at $v >$ 6.50 Å/ps. These investigations may provide some insight into the microcosmic principle of the failure process of polymeric adhesives. © 2009 Wiley Periodicals, Inc. J Appl Polym Sci 115: 460–468, 2010

Key words: adsorption; computer modeling; molecular dynamics; polyethylene (PE)

INTRODUCTION

In industry and daily life, polymer chains are often used as adhesives to agglutinate two parallel surfaces.[1–5] In biology, many junctions between two surfaces are glued by biopolymer chains.[6–8] With the development of advanced single-molecule experimental techniques, such as atomic force microscopy,[8–11] single-molecule force spectroscopy,[12–18] and optical tweezers,[19] the detaching process of two parallel surfaces glued together by a single polymer chain has been explored by the atomic force microscopy experiment.[11] However, the detailed atomistic dynamics and conformational evolution of an adsorbed polymer chain in the experiments are still not quite understood. Fortunately, molecular dynamics simulations[20,21] may play a complementary role in polymeric experiments. A relevant simulation method is the recently developed steered molecular dynamics (SMD) method.[22–36] In this novel simulation technique, an external force is typically applied. However, only one run of SMD simulation was performed in previous investigations. Because of the vast amount of conformation in the polymer chains, it is necessary to check the statistical properties, which were well established in Monte Carlo simulations.[37–45] In this study, the detailed detaching process of two parallel surfaces glued together by a single polyethylene (PE) chains was investigated in combination with the SMD method and Monte Carlo simulations.

Correspondence to: L. Zhang (lxzhang@zju.edu.cn).

Contract grant sponsor: National Natural Science Foundation of China; contract grant numbers: 20574052, 20774066.

Contract grant sponsor: Program for New Century Excellent Talents in University; contract grant number: NCET-05-0538.

Contract grant sponsor: Natural Science Foundation of Zhejiang Province; contract grant numbers: R404047, Y405011, Y405553.

MODEL AND METHODS

Potential model

The united-atom (UA) model of the PE chains was adopted, in which each CH_2 or CH_3 group was regarded as a monomer. In the past 15 years, the UA model of PE chains has been optimized constantly in molecular dynamics simulation.[46–52] In this study, we took the force field of the UA model of the PE chains by Yoon and coworkers,[51,52] which has been parameterized according to first principle calculations and experimental data.

In this force-field model, the total potential energy (U) consists of five parts: the bond-stretching energy (E_{stretch}) for two adjacent monomers, the bond-bending energy (E_{bend}) among three adjacent monomers, the torsion energy (E_{torsion}) among four adjacent monomers, the Lennard–Jones potential (E_{vdw}) between two nonbonded monomers, and the Lennard–Jones adsorption potential (E_{surface}) between each monomer and the attractive surface. E_{stretch} is defined as

$$E_{\text{stretch}} = \sum_{i=2}^{n} \frac{1}{2} k_s (r_i - r_0)^2 \tag{1}$$

where E_{stretch} models an harmonic spring with a bond-stretching constant (k_s) of 634 kcal/(mol Å^2) and an equilibrium bond length (r_0) of 1.53 Å. Here, r_i is the bond length between the adjacent monomers $i - 1$ and i.

E_{bend} is given by

$$E_{\text{bend}} = \sum_{i=3}^{n} \frac{1}{2} k_\theta (\cos\theta_i - \cos\theta_0)^2 \tag{2}$$

where E_{bend} is defined for every triplet of adjacent monomers, k_θ (120 kcal/mol) is the bond-bending constant, θ_0 (1.920) is the equilibrium bond angle, and θ_i represents the bond angle between the bonds $i - 1$ and i.

E_{torsion} is defined as

$$E_{\text{torsion}} = \sum_{i=4}^{n} \frac{1}{2} [k_\phi^1 (1 - \cos\phi_i) + k_\phi^2 (1 - \cos 2\phi_i) + k_\phi^3 (1 - \cos 3\phi_i)] \tag{3}$$

where E_{torsion} is defined for every quadruplet of adjacent monomers and ϕ_i is the dihedral angle between the ($i - 3$,$i - 2$,$i - 1$) plane and the ($i - 2$,$i - 1$,i) plane. The torsion angle constants are $k_\phi^1 = 1.6$ kcal/mol, $k_\phi^2 = -0.867$ kcal/mol, and $k_\phi^3 = 3.24$ kcal/mol.

E_{vdw} is defined as

$$E_{vdw} = \varepsilon \left[\left(\frac{r_m}{r} \right)^{12} - 2 \left(\frac{r_m}{r} \right)^{6} \right] \tag{4}$$

where E_{vdw} is the Van der Waals energy between two nonbonded monomers, which belong to the same chain but are separated by more than three skeletal bonds; ε is a depth parameter of the Lennard-Jones potential; r denotes the distance between the two nonbonded monomers, which is truncated at 9 Å; and r_m (4.5 Å) locates the minimum position in E_{vdw}. The parameter ε depends on the type of the interacting groups, such as CH_2 or CH_3. In the early days of the UA model of the PE chains, ε was taken to be the same for CH_2 and CH_3. The optimized parameters for ε are $\varepsilon_{(CH_2—CH2)} = 0.09344$ kcal/mol, $\varepsilon_{(CH_3—CH3)} = 0.22644$ kcal/mol, and $\varepsilon_{(CH_2—CH3)} = 0.14546$ kcal/mol.

The adsorption energy between the PE chains and the surface is defined as[53,54]

$$E_{\text{surface}} = \sum_{i=1}^{n} w \left[\left(\frac{z_w}{z_i} \right)^9 - \left(\frac{z_w}{z_i} \right)^3 \right] \tag{5}$$

where $z_w = 4.5$ Å is a constant, z_i represents the perpendicular distance between the monomer i and the surface, and w is a parameter to control the adsorption strength. In the simulations reported next, we took a strong adsorption parameter of $w = 6.0$ kcal/mol.[54]

Molecular dynamics method

A schematic illustration of SMD of the detaching process with one of the two adsorption parallel surfaces pulled at a constant pulling velocity (v) is shown in Figure 1. In our model, the lower surface was fixed, whereas the upper surface could be pulled continuously at v. The process modeled a simple failure process of a polymeric adhesive in industry and daily life. In previous reports,[22–36] SMD studies were performed in the v range 0.0001–10.00 Å/ps. In our early work, we commonly chose a low v, such as 0.05 Å/ps.[54] In fact, in some fields, such as the military industry and the aerospace industry, it is necessary that two joined surfaces are fleetly separated by the shock force of an explosion.[55–57] So, in this study, a high v, such as 4.00 Å/

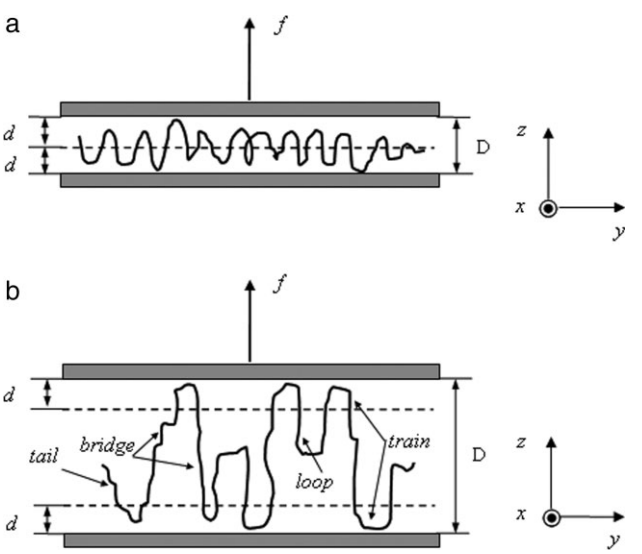

Figure 1 Schematic illustration of SMD of the pulling-off process with one of the two parallel surfaces pulled at a constant v. The tail, bridge, loop, and train represent the microstructures of the chain: (a) the initial conformation with the minimal $D = 2d = 11.6$ Å and (b) one of the conformations during the pulling-off process. f represents the pulling force for the upper surface.

ps, was also explored. Our study may provide some theoretical knowledge for the further application of polymeric adhesives. In Figure 1, D denotes the distance between the two adsorbing parallel surfaces, which was set to 11.6 Å at the beginning of each simulation, that is, $D = 2d = 11.6$ Å in Figure 1(a), where d represents the thickness of the train region on the surface of the chain.

In the molecular dynamics simulation, the positions and velocities of each monomer in the PE chain followed Newton's equation:

$$m_i \frac{d^2\vec{\mathbf{r}}_i}{dt^2} = \vec{F}_i = -\nabla_i U \tag{6}$$

where m_i is the mass of monomer i, $\vec{\mathbf{r}}_i$ denotes the position vector of monomer i, $\vec{F}_i$ is the force on monomer i, and ∇_i is a derivative operator. The adsorption force between the chain and the pulling surface was calculated by

$$f = -\sum_{i=1}^{n} \frac{\partial E_{\text{surface}}}{\partial z_i}. \tag{7}$$

In this study, Beeman's algorithm[58] was used to update the positions and the velocities. The time step was 1 fs. To keep the temperature constant, we scaled the velocities of all monomers by a factor (λ):[54,59]

$$\lambda = \left[1 + \frac{\Delta t}{t_T}\left(\frac{T}{T_c} - 1\right)\right]^{1/2} \tag{8}$$

where T_c is the current kinetic temperature, T denotes the desired temperature, and t_T is a preset time constant ($t_T = 0.4$ ps). Berendsen et al.[59] found that this method was very useful to investigate both the equilibrium and the nonequilibrium processes at a given temperature. The temperature in our simulation was fixed at $T = 280$ K.

Our simulations were carried out *in vacuo* with single PE chains. Simulations *in vacuo* always contain less calculation power because no ions and water molecules have to be calculated. Therefore, simulations *in vacuo* allowed us to explore a larger chain length (N), longer molecular dynamics steps, and a larger number of runs to accumulate statistical data. Many other studies of single PE chains have also been performed *in vacuo* with the molecular dynamics method and the UA model.[49,50,54] The PE N in our simulation was 100, which has been reported in other simulations as well.[54,60,61] In each run, the initial 100-bond single PE chain was set up with a different conformation according to the rotational isomeric state model.[54,62] To make sure that the PE chain reached thermal equilibrium between the two surfaces, 1×10^7 molecular dynamics steps (or 10,000 ps) were implemented first. The upper surface was then lifted at a constant v, and all of the molecular dynamics data were recorded. The procedures were repeated 5000 times in order to improve the precision of our statistical properties.[54]

RESULTS AND DISCUSSION

Chain size and shape

Figure 2 shows the mean-square end-to-end distance ($\langle R^2 \rangle$) as a function of D with different values of v: 0.02, 0.10, 0.50, and 4.00 Å/ps. The value of $\langle R^2 \rangle$ at the beginning, with $D = 11.6$ Å, was the same, 4550 Å^2, for all of the curves. As D increased, the value of $\langle R^2 \rangle$ decreased, which meant that the PE chains folded together. When the velocity was as slow as $v = 0.02$ Å/ps, the chains first folded strongly so that $\langle R^2 \rangle$ dropped to a minimum of 1290.0 Å^2 at $D = 20.8$ Å. As the velocity increased, the minimum value of $\langle R^2 \rangle$ increased, and the position shifted to larger D values. For example, the minimum for $v = 0.10$ Å/ps was 2545.0 Å^2 at $D = 25.7$ Å, whereas it became 2810 Å^2 at $D = 33.5$ Å for $v = 0.50$ Å/ps. A maximum value of $\langle R^2 \rangle = 3361.5$ Å^2 appeared at $D = 67.5$ Å for $v = 0.10$ Å/ps, whereas it was 3853.0 Å^2 at $D = 83.5$ Å for $v = 0.50$ Å/ps. For $v = 4.0$ Å/ps, the maximum disappeared. All curves finally kept the same plateau value of $\langle R^2 \rangle = 3170$ Å^2, which was the equilibrium dimension for the PE chains adsorbed on a single surface. These results showed that the detaching velocity had a strong effect on the conformation evolution of the chain.

The additional dimension properties of the PE chain could be described by the mean-square radius of gyration ($\langle S^2 \rangle$) and the parallel and the perpendicular mean-square radii of gyration ($\langle S^2 \rangle_{xy}$ and $\langle S^2 \rangle_z$, respectively), which are defined as

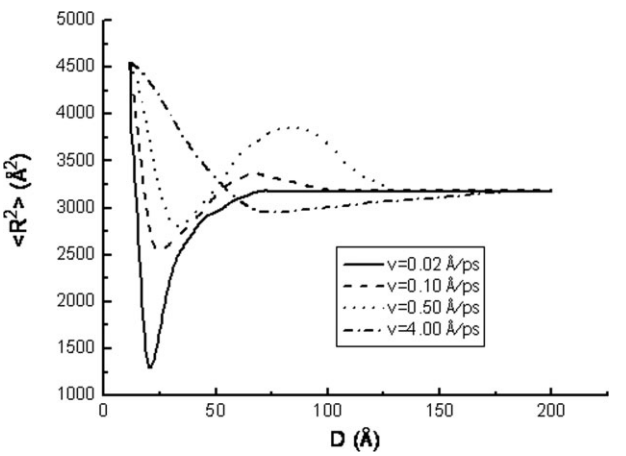

Figure 2 $\langle R^2 \rangle$ as a function of D for the 100-bond PE chains during the pulling-off process with different values of v: 0.02, 0.10, 0.50, and 4.00 Å/ps.

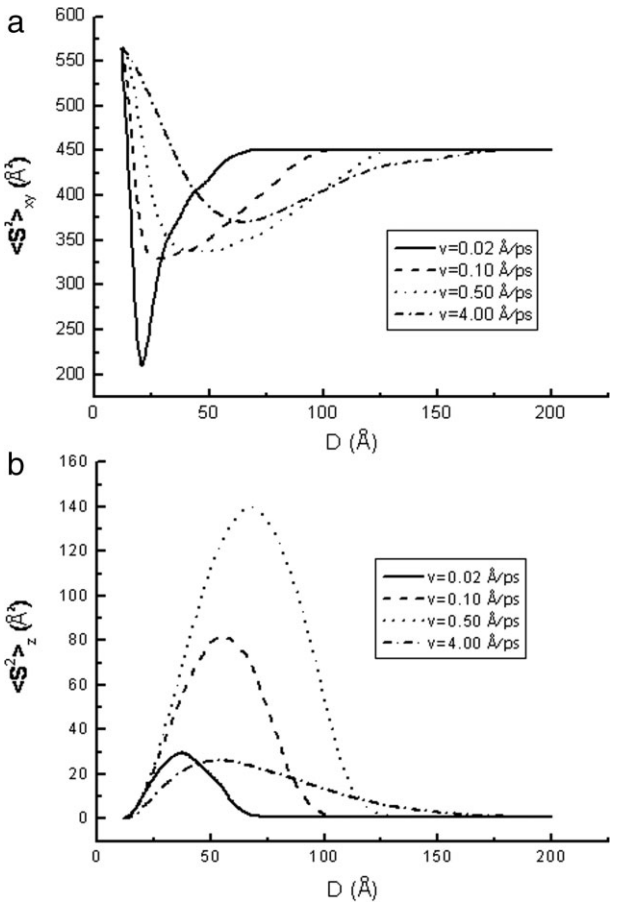

Figure 3 (a) $\langle S^2\rangle_{xy}$ and (b) $\langle S^2\rangle_z$ as a function of D for the 100-bond PE chains during the pulling-off process with different values of v: 0.02, 0.10, 0.50, and 4.00 Å/ps.

$$\langle S^2\rangle_{xy} = \left\langle \frac{1}{N+1}\sum_{i=0}^{N}(x_i - x_{c.m.})^2 + (y_i - y_{c.m.})^2 \right\rangle \quad (9)$$

$$\langle S^2\rangle_z = \left\langle \frac{1}{N+1}\sum_{i=0}^{N}(z_i - z_{c.m.})^2 \right\rangle \quad (10)$$

$$\langle S^2\rangle = \langle S^2\rangle_{xy} + \langle S^2\rangle_z \quad (11)$$

where (x_i, y_i, z_i) are the coordinates of the ith monomer in a chain and $(x_{c.m.}, y_{c.m.}, z_{c.m.})$ is the position of the mass center of a chain. The angular brackets denote the thermodynamic average.

$\langle S^2\rangle_{xy}$ and $\langle S^2\rangle_z$ are plotted in Figure 3 as a function of D with different values of v: 0.02, 0.10, 0.50, and 4.00 Å/ps. The behavior of $\langle S^2\rangle_{xy}$ for different v's was similar: each curve started from the same initial value of $\langle S^2\rangle_{xy}$, 565.0 Å^2; decreased to a minimum; and then rose and subsequently attained a plateau value of $\langle S^2\rangle_{xy} = 450$ Å^2. However, the minimum for each curve was different. It was 209.0 Å^2 for $D = 20.8$ Å with $v = 0.02$ Å/ps, 329.0 Å^2 for $D = 29.5$ Å with $v = 0.10$ Å/ps, 337.0 Å^2 for $D = 45.0$ Å with $v = 0.50$ Å/ps, and 370.0 Å^2 for $D = 66.0$ Å with $v = 4.00$ Å/ps. Figure 3(a) shows that the PE chain first folded itself in the xy plane and then extended into the xy plane when D increased further.

On the other hand, the opposite behavior was observed for $\langle S^2\rangle_z$. Figure 3(b) shows that the PE chain extended itself along the z direction at first. After reaching a maximum, the PE chain detached from one surface and, subsequently, moved toward another surface as D increased still further. The maximum was 30.0 Å^2 for $D = 36.5$ Å with $v = 0.02$ Å/ps, 81.0 Å^2 for $D = 56.0$ Å with $v = 0.10$ Å/ps, 140.0 Å^2 for $D = 67.5$ Å with $v = 0.50$ Å/ps, and 26.0 Å^2 for $D = 52.0$ Å with $v = 4.00$ Å/ps.

Of special interest in Figure 3(b) is the maximum value of $\langle S^2\rangle_z$ for $v = 4.00$ Å/ps, which was even lower than that for $v = 0.02$ Å/ps. To check where the turning point was, the relationship between the maximum value of the perpendicular mean-square radius of gyration ($\langle S^2\rangle_{z,\max}$) and v was studied in detail, as shown in Figure 4. The range of v explored here was 0.005–8.0 Å/ps. When $v < 0.01$ Å/ps or $v > 6.0$ Å/ps, $\langle S^2\rangle_{z,\max}$ was small and depended weakly on v. However, in the range $v = 0.01$–6.0 Å/ps, two regions of distinctive behavior could be identified. The data points fell on two distinctive lines, which could be fitted to

$$\langle S^2\rangle_{z,\max} = \mathrm{A}(\log_{10} v) + B \quad (12)$$

with $A = 93.3$ and $B = 182.7$ for $v = 0.01$–3.0 Å/ps and $A = -1077.9$ and $B = 723.6$ for $v = 3.0$–6.0 Å/ps. The two lines crossed each other at $v = 3.0$ Å/ps (labeled in Fig. 4). Here A and B are linear fitting parameter.

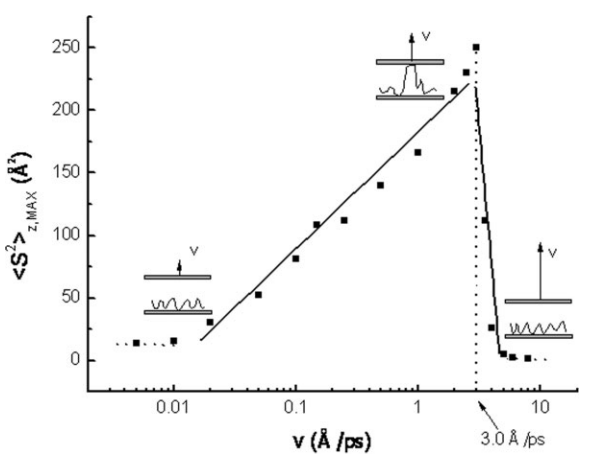

Figure 4 $\langle S^2\rangle_{z,\max}$ as a function of v (in the logarithmic scale). The data points are our simulation results, and the solid lines are the fitting results from eq. (12). The three inset figures represent three possible conformations with different v's.

When v was small enough, such as $v = 0.02$ Å/ps, the PE chain could be early adsorbed only onto a single surface because the speed of the detachment of the PE chain from the adsorption surface exceeded the separate speed of the two surfaces, and this led to a small value of $\langle S^2 \rangle_{z,\max}$. When v increased, $\langle S^2 \rangle_{z,\max}$ increased gradually and reached a maximum value of $\langle S^2 \rangle_{z,\max} = 250$ Å^2 at $v = 3.0$ Å/ps. However, because the adsorption force between the PE chain and the pulling surface was limited, when v was larger than 3.0 Å/ps, the PE chain started to fall behind the movement of the detaching surface. So, when v was large enough, such as $v = 4.0$ Å/ps, the chain detached from the pulling surface at an early stage. To illustrate the behavior, we added three insets to show possible conformations in Figure 4.

Now, let us consider the tensor (**S**), defined as

$$\mathbf{S} = \frac{1}{N+1}\sum_{i=0}^{N} S_i S_i^T = \begin{pmatrix} S_{xx} & S_{xy} & S_{xz} \\ S_{yx} & S_{yy} & S_{yz} \\ S_{zx} & S_{zy} & S_{zz} \end{pmatrix} \tag{13}$$

where $S_i = \mathrm{col}(x_i, y_i, z_i)$ denotes the position of monomer i in a frame of reference with its origin at the center of mass and *Si(T)* is the transpose of the matrix *Si*. The tensor **S** can be diagonalized to give three eigenvalues of L_1^2, L_2^2, and L_3^2 ($L_1^2 \le L_2^2 \le L_3^2$). Solc and Stockmayer[60,61] found that the ratio of the parameters ($\langle L_1^2 \rangle : \langle L_2^2 \rangle : \langle L_3^2 \rangle$) characterized the shape of the polymer chain, and they obtained a ratio of 1 : 2.7 : 11.7 on the basis of a random walk of 100 bonds in a simple cubic lattice. With the three eigenvalues for the tensor **S**, a new parameter[63,64] characteristic of the shape of the chain can be defined as

$$\langle \delta \rangle = 1 - 3\left\langle \frac{L_1^2 L_2^2 + L_2^2 L_3^2 + L_1^2 L_3^2}{(L_1^2 + L_2^2 + L_3^2)^2} \right\rangle \tag{14}$$

where $\langle \delta \rangle$ is the shape factor, which varies between 0 and 1. When it is 0, the shape of the chain is a sphere. When it is 1, the shape of the chain is a rod. The shape of the chain is spheroid when $\langle \delta \rangle$ is between 0 and 1. Thus, $\langle \delta \rangle$ gives quantitative information of the shape.

$\langle \delta \rangle$ as a function of D is plotted in Figure 5. Starting from the same initial value of $\langle \delta \rangle = 0.79$, all curves first decreased to a minimum value, then increased, and subsequently attained a plateau value of $\langle \delta \rangle = 0.75$. The minimum value was 0.55 for $D = 22.0$ Å at the small velocity of $v = 0.02$ Å/ps, 0.59 for $D = 31.2$ Å at $v = 0.10$ Å/ps, 0.61 for $D = 37.8$ Å at $v = 0.50$ Å/ps, and 0.70 for $D = 64.0$ Å at $v = 4.00$ Å/ps. When Figure 3(b) is compared with Figure 5, the tendencies of $\langle \delta \rangle$ and $\langle S^2 \rangle_z$ appear to be similar. To illustrate the behavior, four insets for possible shapes are displayed in Figure 5. At the beginning of the detaching process, the PE chains were condensed between the two adsorption surfaces. When D increased, the PE chains elongated in the z direction and, at the same time, shrank in the xy plane. When the chain $\langle \delta \rangle$'s reached the minimum, the chains had the shape of a prolate spheroid for $v = 0.02$, 0.1, and 0.5 Å/ps. However, in the case of $v = 4.0$ Å/ps, the PE chain detached itself from one surface at an early stage. For all cases, the PE chains eventually came back to one surface.

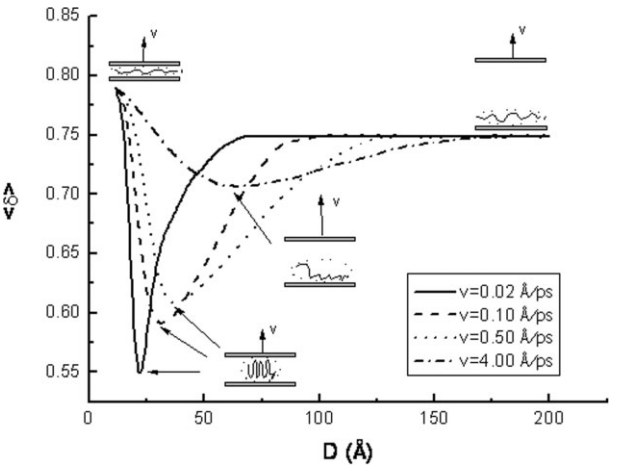

Figure 5 $\langle \delta \rangle$ as a function of D for the 100-bond PE chains during the pulling-off process with different values of v: 0.02, 0.10, 0.50, and 4.00 Å/ps. The four inset figures represent four possible shapes with different v's and different values of D.

Microstructure of the chain

The conformation of the chain could also be further analyzed through the segment density distribution [$\langle f(z) \rangle$], which is defined as

$$f(z) = \frac{N(z)}{N+1} \tag{15}$$

where $N(z)$ is the number of monomers in the layer at a distance z from reference surface. In this study, the reference surface was the lower surface, and the thickness of each layer was 1 Å. In Figure 6, $\langle f(z) \rangle$ is plotted as a function of z for the PE chains with different values of v: 0.02, 0.10, 0.50, and 4.00 Å/ps, respectively. Figure 6(a–c) shows the results at different distances of D: 30, 60, and 90 Å, respectively.

At the beginning of the detaching process, the PE chains were condensed between the two surfaces. After 1×10^7 molecular dynamics steps (or 10,000 ps) were implemented at room temperature ($T = 280$ K), the PE chain reached thermal equilibrium. In this study, Berendsen et al.'s[59] heat constraint algorithm was used to fix the T_c of the system. The average thermal motion speed of the monomer (v_T) was 7.06 Å/ps at room temperature ($T = 280$ K). Then,

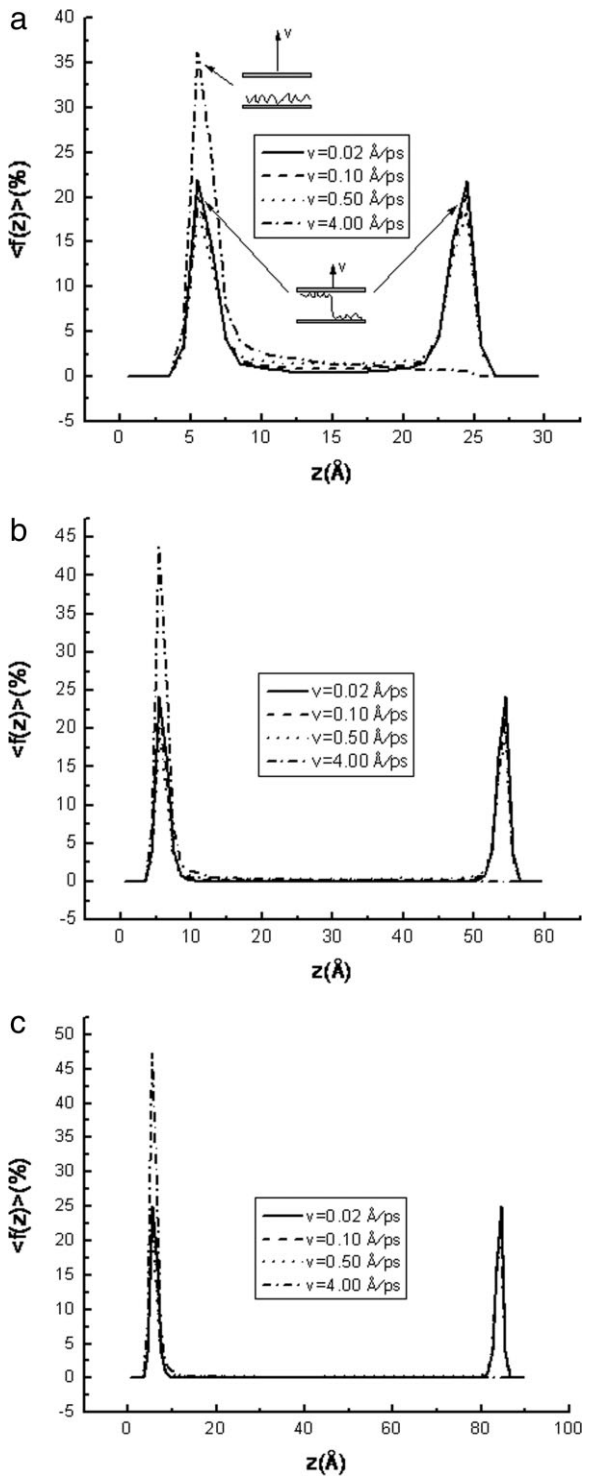

Figure 6 $\langle f(z)\rangle$ as a function of z for the PE chains during the pulling-off process with different values of v: 0.02, 0.10, 0.50, and 4.00 Å/ps. D = (a) 30, (b) 60, and (c) 90 Å.

the upper surface was lifted at a constant velocity. Because the pulling up to the PE chain more or less led to an increase in the average kinetic energy of the monomer, the background heat constraint of the system hindered the increasing v_T. Under low v, such as v = 0.02, 0.10, and 0.50 Å/ps, the constraint effect was inconspicuous; the monomers were equally distributed on the two surfaces. Therefore, the curves with v = 0.02, 0.10, and 0.50 Å/ps are nearly symmetrical in Figure 6. However, the high v (4.00 Å/ps) was even close to v_T at room temperature (T = 280 K). If the PE chain attempted to catch up with the quickly moving upper surface, it had to overcome the high heat friction from the heat constraint. Because the adsorption force between the PE chain and the upper surface was limited, the PE chain finally dropped to lower surface. So, the curve with v = 4.00 Å/ps is asymmetrical in Figure 6, which means that the monomers were only distributed on the lower surface. As D increased from 30 to 90 Å [see Fig. 6(a–c)], the peaks became sharper, which means that the monomers aggregated near the surfaces. In Figure 6(a), we show the different conformations at large and small velocities in the insets.

The microstructure of the chain could also be analyzed through the tail, train, bridge, and loop structures of segments,[1] as shown in Figure 1(b). When the two ends of a segment are adsorbed on two different surfaces or the same surface, the segment is called a *bridge* or a *loop* structure. The tail structure is formed when only one end of the segment is adsorbed onto the surface and the other remains unanchored. The train structure is formed when all monomers of the segment are adsorbed onto the surface. Figure 7 displays the average percentage of the microstructure of the chain [(a) $\langle P_{\text{tail}}\rangle$, (b) $\langle P_{\text{train}}\rangle$, (c) $\langle P_{\text{bridge}}\rangle$, and (d) $\langle P_{\text{loop}}\rangle$ (where the subscript denotes the structure of the chain)] as a function of D for the 100-bond PE chains during the detaching process with different values of v: 0.02, 0.10, 0.50, and 4.00 Å/ps. At the beginning of the detaching process, the distance between the two surfaces was $D = D_{\text{min}} = 2d$ = 11.6 Å [see Fig. 1(a)]. Here, D_{min} represents the minimal distance between two surface in our simulation. All of the monomers of the chain fell in the train layers; therefore, the monomers in the tail, bridge, and loop structures were zero. When D slightly increased, the values of $\langle P_{\text{tail}}\rangle$, $\langle P_{\text{bridge}}\rangle$, and $\langle P_{\text{loop}}\rangle$ increase, and the value of $\langle P_{\text{train}}\rangle$ decreased. When D increased further, the value of $\langle P_{\text{train}}\rangle$ rebounded and then attained a plateau value of 41.1%; the value of $\langle P_{\text{loop}}\rangle$ increased steadily and subsequently attained a plateau value of 52.5%, whereas the value of $\langle P_{\text{bridge}}\rangle$ decreased to zero. It was obvious that the chain had moved toward a single surface when $\langle P_{\text{bridge}}\rangle$ decreased to zero. For $\langle P_{\text{tail}}\rangle$, it rose to a maximum before it dropped to a plateau value of 6.4%.

Thermodynamic properties

For the thermodynamic properties, we calculated the average surface adsorption energy ($\langle E_{\text{surface}}\rangle$), the average total energy ($\langle U\rangle$), and the average pulling force ($\langle f\rangle$). Figure 8 displays $\langle E_{\text{surface}}\rangle$ and $\langle U\rangle$ as

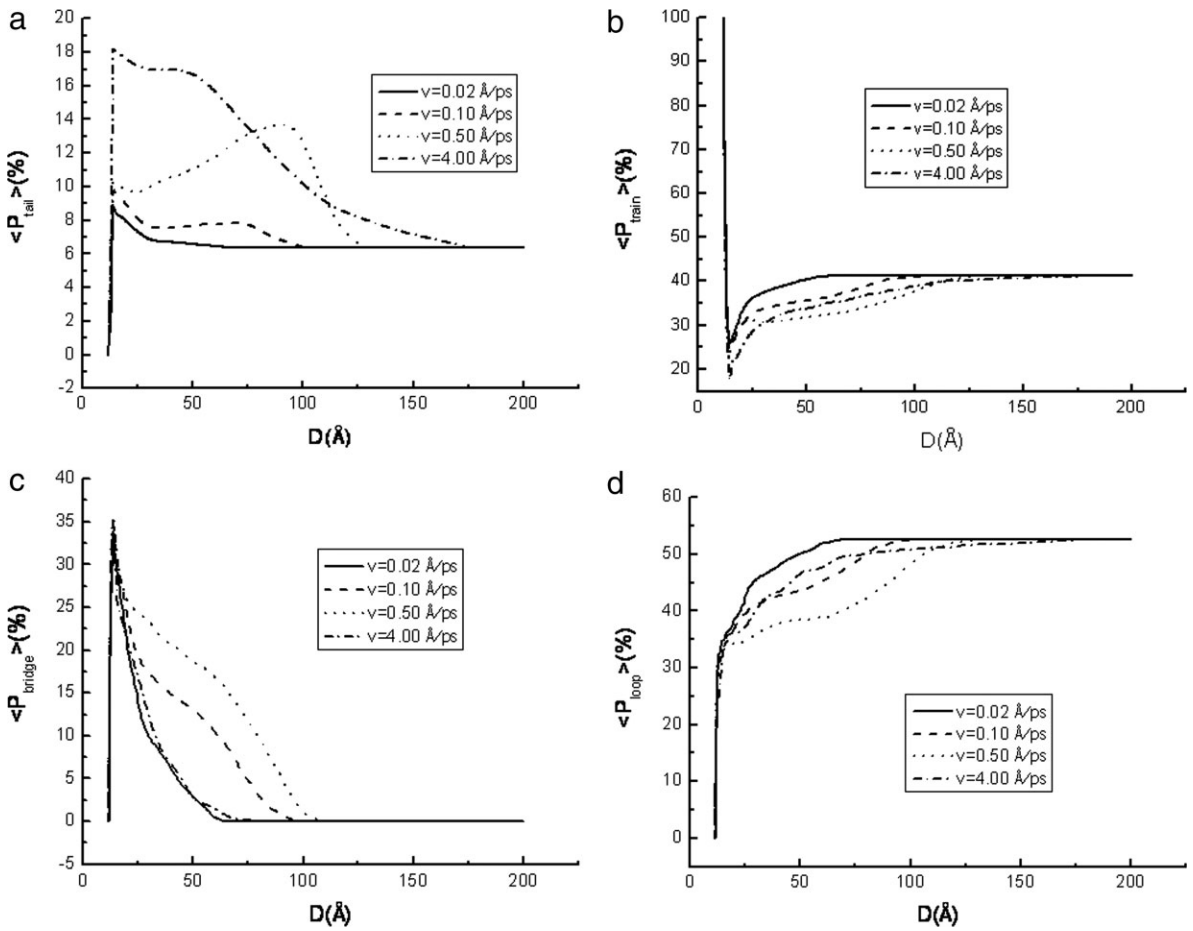

Figure 7 Average percentage of the microstructure of the chain, (a) $\langle P_{\text{tail}} \rangle$, (b) $\langle P_{\text{train}} \rangle$, (c) $\langle P_{\text{bridge}} \rangle$, and (d) $\langle P_{\text{loop}} \rangle$, as a function of D for the 100-bond PE chains during the pulling-off process with different values of v: 0.02, 0.10, 0.50, and 4.00 Å/ps.

function of D for the 100-bond PE chains during the detaching process with different values of v: 0.02, 0.10, 0.50, and 4.00 Å/ps, respectively. As shown in Figure 8(a), $\langle E_{\text{surface}} \rangle$ started from an initial value of $= -419.8$ kcal/mol, increased to a maximum value, and then decreased to a plateau value of $\langle E_{\text{surface}} \rangle = -193.0$ kcal/mol. The maximum value of $\langle E_{\text{surface}} \rangle$ depended on the velocity. It was -184.0 kcal/mol for $D = 30.5$ Å at $v = 0.02$ Å/ps, -171.0 kcal/mol for $D = 43.5$ Å at $v = 0.10$ Å/ps, -157.0kal/mol for $D = 49.0$ Å at $v = 0.50$ Å/ps, and -163.0 kcal/mol for $D = 32.5$ Å at $v = 4.00$ Å/ps. At the beginning of the detaching process, the PE chain was tightly confined between two surfaces, so the surface adsorption energy was minimum.

On the other hand, the total energy was the sum of the surface adsorption energy, the kinetic energy of all monomers, the potential energies related to bond lengths, bond angles, and torsion angles, and the nonbonded energy. As shown in Figure 8(b), $\langle U \rangle$ started from an initial value of -261.0 kcal/mol, increased to a maximum, and then decreased to a plateau value of $\langle U \rangle = -32.0$ kcal/mol. The maximum value was -23.0 kcal/mol for $D = 30.5$ Å at $v = 0.02$ Å/ps, -10.5 kcal/mol for $D = 43.5$ Å at $v = 0.10$ Å/ps, 4.5 kcal/mol for $D = 49.0$ Å at $v = 0.50$ Å/ps, and -3.0 kcal/mol for $D = 32.5$ Å at $v = 4.00$ Å/ps. The behavior of $\langle U \rangle$ was similar to $\langle E_{\text{surface}} \rangle$, because the total energy was mainly contributed from the surface adsorption energy under conditions of the strong adsorption.

Figure 9 displays $\langle f \rangle$ as a function of D during the detaching process with different values of v: 0.02, 0.10, 0.50, and 4.00 Å/ps, respectively. The negative value at the beginning means that the PE chain was under compression. As D increased slightly, $\langle f \rangle$ rose abruptly to reach a peak value. As D increased still further, $\langle f \rangle$ decreased until it reached zero, when the chain detached from one of two surfaces. Interestingly, in our previous simulation of the pulling the PE chain directly from single adsorbing surface, a force plateaus was observed.[54]

The relationship between the peak value of the force ($\langle f \rangle_{\max}$) and v is shown in Figure 10. The points are the simulation results in Figure 10; the curve was fitted to the following expression:

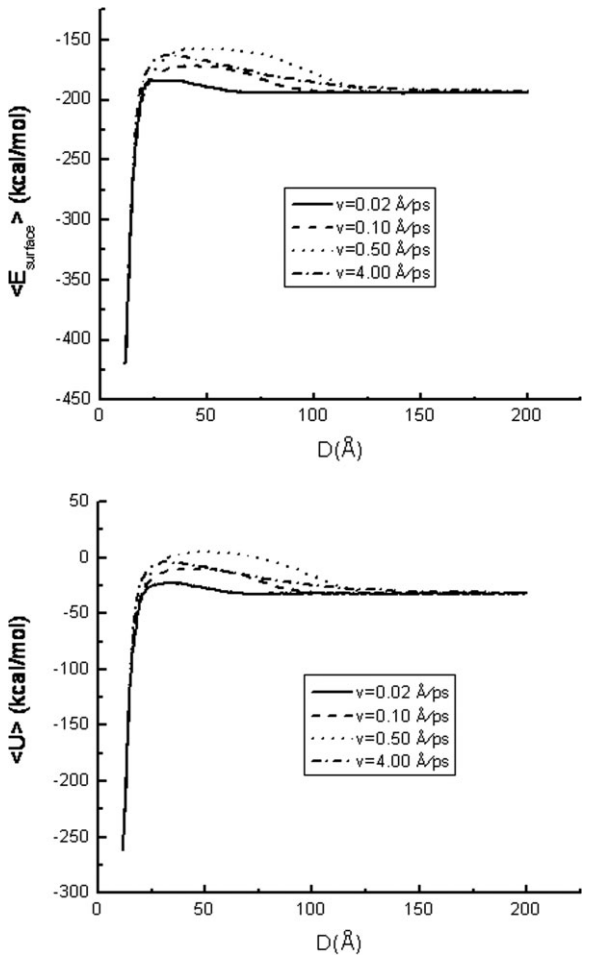

Figure 8 (a) $\langle E_{surface} \rangle$ and (b) $\langle U \rangle$ as a function of D for the 100-bond PE chains during the pulling-off process with different values of v: 0.02, 0.10, 0.50, and 4.00 Å/ps.

$$\langle f \rangle_{max} = a^{\log_{10}(bv)+c} + d \tag{16}$$

with $a = 2.6$, $b = 3000.0$, $c = 2.3$, and $d = 820.0$. When v was less than 10^{-2} Å/ps, $\langle f \rangle_{max}$ depended weakly on v. As v tended to zero, $\langle f \rangle_{max}$ tended to a fixed value of 820.0 pN. Experimental scientists believed that the detaching process under the low velocity was close to the equilibrium process.[15] At 10^{-2} Å/ps $< v <$ 6.50 Å/ps, $\langle f \rangle_{max}$ rose sharply. However, when v was more than 6.50 Å/ps, $\langle f \rangle_{max}$ deviated from eq. (16) and attained a stable value of $\langle f \rangle_{max}$ of 1390 pN. In the model, the strength of the pulling force depended on the amount of the chain bridges between two surfaces. The more the chain bridges were formed between two surfaces, the stronger the pulling force was that lifted upper surface. As shown in Figure 9, the peak values of the force all occurred at the initial pulling stage of $D =$ 13 Å because the most chain bridges were formed between two surfaces at that time. However, because of the limitation of N, the amount of the chain bridges formed were finite. Furthermore, the adsorption force between the PE chain and the upper surface also was limited. Therefore, $\langle f \rangle_{max}$ retained a stable maximum of $\langle f \rangle_{max} = 1390$ pN at $v > 6.50$ Å/ps. In ref. 54, the single PE chain was pulled up from its end. In the pulling process, the monomers of the PE chain were detached from the adsorbing surface one by one. The pulling force measured was only the detaching force between the single monomers on the chain and the surface; as such, the pulling force did not depend on N. Therefore, a force plateau was observed and was shown in Figure 8 of ref. 54. In our model, the pulling force depends on the amount of the chain bridges between two surfaces, which is equivalent to that of many single chains in ref. 54 pulled up together. So the values of $\langle f \rangle_{max}$ in Figure 10 are about 10 times larger than those the pulling

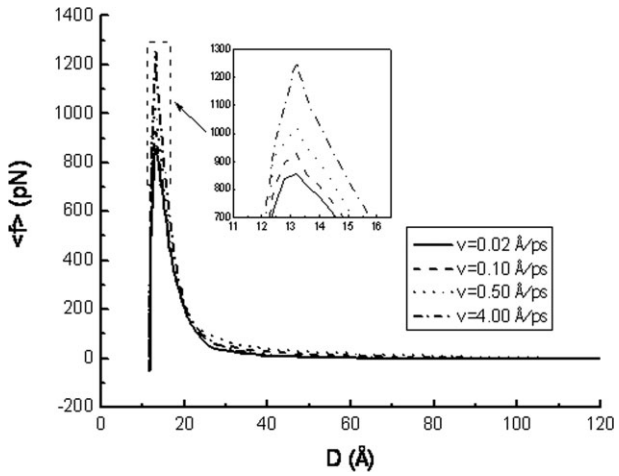

Figure 9 $\langle f \rangle$ as a function of D for the 100-bond PE chains during the pulling-off process with different values of v: 0.02, 0.10, 0.50, and 4.00 Å/ps.

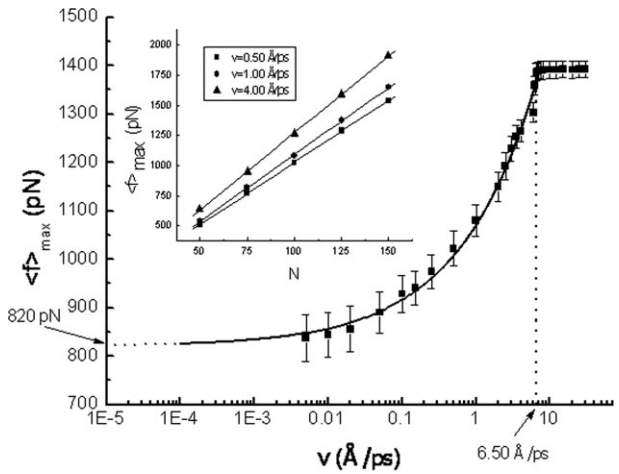

Figure 10 $\langle f \rangle_{max}$ as a function of v (in the logarithmic scale). The points are the simulation results, and the solid line and the dotted line, respectively represent the fitting by eq. (16) and the extrapolation from it. The inset figure shows $\langle f \rangle_{max}$ as a function of N with different values of v: 0.50, 1.00, and 4.00 Å/ps.

force in Figure 9 of ref. 54. In addition, we added an inset figure in Figure 10, which shows $\langle f \rangle_{max}$ as a function of N with different values of v: 0.50, 1.00 and 4.00 Å/ps. There always existed an increasing linear relationship for $\langle f \rangle_{max}$ versus N because the amount of the chain bridges formed depended on N.

CONCLUSIONS

We report the SMD simulation of the detaching process of two surfaces glued together by a single PE chain *in vacuo*. $\langle R^2 \rangle$, $\langle S^2 \rangle$, and $\langle \delta \rangle$ were analyzed to characterize the conformational change during the detaching process. $\langle S^2 \rangle_{z,max}$ as a function of v showed two regions of distinctive behavior with the turning point at $v = 3.0$ Å/ps. $\langle f(z) \rangle$ showed that it was difficult to distribute symmetrically on two surfaces with a high v, such as $v = 4.0$ Å/ps. The maximum pulling force weakly depended on v at $v < 10^{-2}$ Å/ps, whereas it rose sharply as v is 10^{-2} Å/ps $< v <$ 6.50 Å/ps. However, when v was more than 6.50 Å/ps, $\langle f \rangle_{max}$ retained a stable value. Our results may provide some insight into related processes and further investigations for polymeric adhesives.

References

1. Ha, B.; Char, K. Langmuir 2005, 21, 8471.
2. Lee, W. J.; Lin, M. S. J Appl Polym Sci 2008, 109, 23.
3. Maandi, E.; Sung, C. S. P. J Appl Polym Sci 2008, 107, 3685.
4. Jung, J. S.; Kim, J. H.; Kim, M. S.; Jeong, H. M.; Kim, Y. S.; Kim, T. K.; Hwang, J. M.; Lee, S. Y.; Cho, Y. L. J Appl Polym Sci 2008, 109, 1757.
5. Moon, S.; Swearingen, S.; Foster, M. D. Polymer 2004, 45, 5951.
6. Blawas, A. S.; Reichert, W. M. Biomaterials 1998, 19, 595.
7. Deming, T. J. Prog Polym Sci 2007, 32, 858.
8. Carrion-Vazquez, M.; Oberhauser, A. F.; Fisher, T. E.; Marszalek, P. E.; Li, H. B.; Fernandez, J. M. Prog Biophys Mol Biol 2000, 74, 63.
9. Binning, G.; Quate, C. F.; Gerber, C. Phys Rev Lett 1986, 56, 930.
10. Bemis, J.; Akhremitchev, B.; Walker, G. Langmuir 1999, 15, 2799.
11. Sonnenberg, L.; Parvole, J.; Kühner, F.; Billon, L.; Gaub, H. E. Langmuir 2007, 23, 6660.
12. Rief, M.; Oesterhelt, F.; Heymann, B.; Gaub, H. E. Science 1997, 275, 1295.
13. Rief, M.; Gautel, M.; Oesterhelt, F.; Fernandz, J. M.; Gaub, H. E. Science 1997, 276, 1109.
14. Kühner, F.; Erdmann, M.; Gaub, H. E. Phys Rev Lett 2006, 97, 218301.
15. Cui, S. X.; Liu, C. J.; Zhang, X. Nano Lett 2003, 3, 245.
16. Wang, C.; Shi, W. Q.; Zhang, W. K.; Zhang, X.; Katsumoto, Y.; Ozaki, Y. Nano Lett 2002, 2, 1169.
17. Janshoff, A.; Neitzert, M.; Oberdorf, Y.; Fuchs, H. Angew Chem Int Ed 2000, 39, 3212.
18. Hugel, T.; Seitz, M. Macromol Rapid Commun 2001, 22, 989.
19. Lavery, R.; Lebrun, A.; Allemand, J. F.; Bensimon, D.; Croquette, V. J Phys Condens Matter 2002, 14, R383.
20. Jawalkar, S. S.; Nataraj, S. K.; Raghu, A. V.; Aminabhavi, T. M. J Appl Polym Sci 2008, 108, 3572.
21. Sikdar, D.; Katti, D. R.; Katti, K. S. J Appl Polym Sci 2008, 107, 3137.
22. Izrailev, S.; Crofts, A. R.; Berry, E. A.; Schulten, K. Biophys J 1999, 77, 1753.
23. Wriggers, W.; Schulten, K. Proteins Struct Funct Genes 1999, 35, 262.
24. Lu, H.; Schulten, K. Chem Phys 1999, 247, 141.
25. Marszalek, P. E.; Lu, H.; Li, H.; Carrion-Vazquez, M.; Oberhauser, A. F.; Schulten, K.; Fernandez, J. M. Nature 1999, 402, 100.
26. Gao, M.; Wilmanns, M.; Schulten, K. Biophys J 2002, 83, 3435.
27. Gullingsrud, J.; Schulten, K. Biophys J 2003, 85, 2087.
28. Grubmüller, H.; Heymann, B.; Tavan, P. Science 1996, 271, 997.
29. Heymann, B.; Grubmüller, H. Chem Phys Lett 1999, 303, 1.
30. Heymann, B.; Grubmüller, H. Chem Phys Lett 1999, 307, 425.
31. Gräter, F.; Shen, J.; Jiang, H.; Gautel, M.; Grubmüller, H. Biophys J 2005, 88, 790.
32. Xu, Y.; Shen, J.; Luo, X;,Silman, I.; Sussman, J. L.; Chen, K.; Jiang, H. J Am Chem Soc 2003, 125, 11340.
33. Isralewitz, B.; Gao, M.; Schulten, K. Curr Opin Struc Bio 2001, 11, 224.
34. Kosztin, D.; Izrailev, S.; Schulten, K. Biophys J 1999, 76, 188.
35. Lu, H.; Isralewitz, B.; Krammer, A.; Vogel, V.; Schulten, K. Biophys J 1998, 75, 662.
36. Izrailev, S.; Stepaniants, S.; Isralewitz, B.; Kosztin, D.; Lu, H.; Molnar, F.; Wriggers, W.; Schulten, K. Computational Molecular Dynamics: Challenges, Methods, Ideas; Springer-Verlag: Berlin, 1998.
37. Grassberger, P. Phys Rev E 1997, 56, 3682.
38. Frauenkron, H.; Bastolla, U.; Gerstner, E.; Grassberger, P.; Nadler, W. Phys Rev Lett 1998, 80, 3149.
39. Hus, H. P.; Mehra, V.; Nadler, W.; Grassberger, P. Phys Rev E 2003, 68, 021113.
40. Hus, H. P.; Mehra, V.; Nadler, W.; Grassberger, P. J Chem Phys 2003, 118, 444.
41. Zhang, L. X.; Su, J. Y. Polymer 2006, 47, 735.
42. Shen, Y.; Zhang, L. X. Polymer 2007, 48, 3593.
43. Shen, Y.; Zhang, L. X. J Polym Sci Part B: Polym Phys 2005, 43, 223.
44. Yi, W. Q.; Zhang, L. X. Eur Polym J 2006, 42, 573.
45. Sun, T. T.; Zhang, L. X.; Chen, J.; Shen, Y. J Chem Phys 2004, 120, 5469.
46. Liao, Q.; Jin, X. J Chem Phys 1999, 110, 8835.
47. Fujiwara, S.; Sato, T. J Chem Phys 1997, 107, 613.
48. Koyama, A.; Yamamoto, T.; Fukao, K.; Miyamoto, Y. J Chem Phys 2001, 115, 560.
49. Fujiwara, S.; Sato, T. J Chem Phys 2001, 114, 6455.
50. Doran, M.; Choi, P. J Chem Phys 2001, 115, 2827.
51. Chang, J.; Han, J.; Yang, L.; Jaffe, R. L.; Yoon, D. Y. J Chem Phys 2001, 115, 2831.
52. Hur, K.; Winkler, R. G.; Yoon, D. Y. Macromolecules 2006, 39, 3975.
53. Celestini, F.; Frisch, T.; Oyharcabal, X. Phys Rev E 2004, 70, 012801.
54. Wang, Y.; Zhang, L. X. J Polym Sci Part B: Polym Phys 2007, 45, 2322.
55. Thomas, C. L. S&V Bull 1973, 43(1). 119.
56. Hughes, M. E. S&V Bull 1983, 53(1). 83.
57. Moening, C. J. S&V Bull 1986, 56(3). 3.
58. Beeman, D. J Comp Phys 1976, 20, 130.
59. Berendsen, H. J. C.; Postma, J. P. M.; Gunsteren, V.; Dinola, A.; Haak, J. R. J Chem Phys 1984, 81, 3684.
60. Solc, K. J Chem Phys 1971, 55, 335.
61. Solc, K.; Stockmayer, W. H. J Chem Phys 1971, 54, 2756.
62. Fukuda, M. J Chem Phys 1998, 109, 6476.
63. Zifferer, G.; Preusser, W. Macromol Theory Simul 2001, 10, 397.
64. Jagodzinski, O.; Eisenriegler, E.; Kremer, K. J Phys I 1992, 2, 2243.